

10-2-2000

Nanostructured FePt:B₂O₃ thin films with perpendicular magnetic anisotropy

C.P. Luo

University of Nebraska - Lincoln

Sy_Hwang Liou

University of Nebraska-Lincoln, sliou@unl.edu

L. Gao

University of Nebraska - Lincoln

Yi Liu

University of Nebraska-Lincoln, yliu@unl.edu

David J. Sellmyer

University of Nebraska-Lincoln, dsellmyer@unl.edu

Follow this and additional works at: <http://digitalcommons.unl.edu/physicsliou>



Part of the [Physics Commons](#)

Luo, C.P.; Liou, Sy_Hwang; Gao, L.; Liu, Yi; and Sellmyer, David J., "Nanostructured FePt:B₂O₃ thin films with perpendicular magnetic anisotropy" (2000). *Si-Hwang Liou Publications*. 65.
<http://digitalcommons.unl.edu/physicsliou/65>

This Article is brought to you for free and open access by the Research Papers in Physics and Astronomy at DigitalCommons@University of Nebraska - Lincoln. It has been accepted for inclusion in Si-Hwang Liou Publications by an authorized administrator of DigitalCommons@University of Nebraska - Lincoln.

Nanostructured FePt:B₂O₃ thin films with perpendicular magnetic anisotropy

C. P. Luo, S. H. Liou, and L. Gao

Behlen Laboratory of Physics and Center for Materials Research and Analysis, University of Nebraska, Lincoln, Nebraska 68588-0111

Y. Liu

Department of Mechanical Engineering and Center for Materials Research and Analysis, University of Nebraska, Lincoln, Nebraska 68588-0656

D. J. Sellmyer^{a)}

Behlen Laboratory of Physics and Center for Materials Research and Analysis, University of Nebraska, Lincoln, Nebraska 68588-0111

(Received 24 April 2000; accepted for publication 3 August 2000)

FePt/B₂O₃ multilayers were deposited by magnetron sputtering onto 7059 glass substrates. By annealing the as-deposited films at 550 °C, nanostructured FePt:B₂O₃ films consisting of FePt grains with *L*1₀ structure, embedded in a glassy B₂O₃ matrix, were obtained. The *c* axes of the FePt grains can be made to align with the film normal direction, which results in a perpendicular anisotropy constant of 3.5×10^7 erg/cc. The films remain layered structures after annealing when the B₂O₃ layer thickness exceeds 16 Å. The nanostructure of the films was investigated by transmission electron microscopy. The coercivities and the average grain sizes of the films are dependent on the B₂O₃ concentrations, with coercivities varying from 4 to 12 kOe, while average grain sizes vary from 4 to 17 nm. Strong perpendicular anisotropy, adjustable coercivity, and fine grain size suggest this nanocomposite system might have significant potential as recording media at extremely high areal density. © 2000 American Institute of Physics. [S0003-6951(00)01540-0]

The growth mechanism, magnetic, and structural properties of FePt equiatomic alloy thin films with the *L*1₀ ordered structures are of great interest from both scientific and application viewpoints. They are potential high-density recording media¹⁻³ and high-energy permanent magnets⁴ because of their exceptional magnetic properties. The essential feature is that they can undergo a phase transition from the disordered face-centered cubic (fcc) structure to the ordered face-centered tetragonal (fct) structure (*L*1₀ phase) after post-deposition annealing,¹ or when deposited at an elevated substrate temperature.⁵ The long-range ordering has critical effects on the magnetic properties of the films.⁶ It is well known that the ordered FePt alloy has a very high anisotropy constant *K*₁ of 7×10^7 erg/cc,⁷ and recently *K*₁ values greater than 10^8 erg/cc were found in fully ordered FePt films grown by molecular beam epitaxy (MBE).^{8,9} FePt thin films deposited by magnetron sputtering tend to grow with a (111) texture, placing the *c* axes of the grains at an angle of 36° above the film plane.² By applying the MBE technique, FePt can grow epitaxially on MgO (001) single-crystal substrates with the *c* axes of the grains in the film normal direction, resulting in perpendicular magnetic anisotropy.^{5,8,9} However, this requires complex MBE technology and MgO single crystals as substrates. In this research, we successfully deposited the FePt:B₂O₃ nanocomposite thin films on 7059 glass substrates, which consist of nanometer size, *L*1₀ structured FePt particles embedded in a B₂O₃ matrix. The *c* axes

of the particles are aligned along the film normal direction. The magnetic and structural properties of these films were investigated.

FePt/B₂O₃ multilayers were deposited on 7059 glass substrates by dc- and rf-magnetron sputtering. The base pressure of the sputtering chamber was 2×10^{-7} Torr and high purity Ar was used for deposition at a pressure of 5 mTorr. A composite FePt target was made by putting some Fe chips (99.99% purity) on the Pt target (99.99% purity). The composition of the FePt target was adjusted by the number of Fe chips. The B₂O₃ target with a purity of 99.9% was obtained from Target Materials, Inc. The as-deposited films were annealed in vacuum at 550 °C for 30 min. The structure of the films was investigated by transmission electron microscopy (TEM) and x-ray diffraction (XRD) with Cu *K*α radiation. Magnetic properties were measured by a Quantum Design superconducting quantum interference device. Domain patterns were observed with a magnetic force microscope (MFM).

(FePt 32 Å/B₂O₃ *x* Å)₅ multilayers with *x* varying from 4 to 48 Å were deposited with the glass substrates held at ambient temperatures. The as-deposited films contain a disordered fcc FePt phase and are magnetically soft with coercivity less than 100 Oe. After annealing at 550 °C, the Fe–Pt undergoes a phase transition from the disordered fcc to the ordered fct structure, which is characterized by the (001) and (002) superlattice peaks of the XRD scans, as shown in Fig. 1. Compared with the FePt single-layer film, the intensity of the (111) diffraction peaks decreases as the B₂O₃ layer thickness increases in the FePt/B₂O₃ multilayers. As the B₂O₃ layer thickness increases to 12 Å and above, the (111) peak

^{a)}Author to whom correspondence should be addressed; electronic mail: dsellmyer@unl.edu

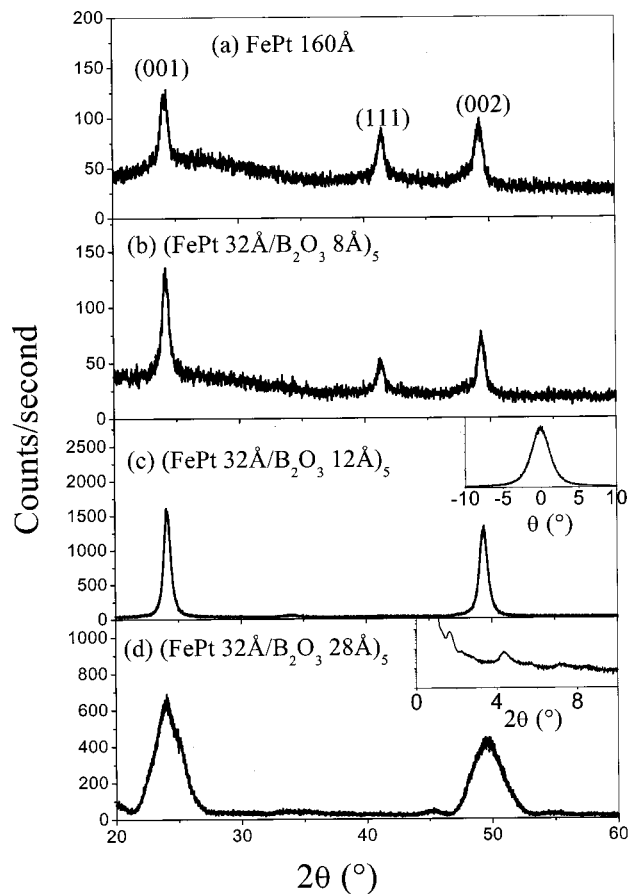


FIG. 1. XRD θ - 2θ scans. The inset in (c) and (d) are the (001) peak rocking curve and the low angle θ - 2θ scan, respectively.

disappears while the (001) and (002) peaks dominate, which implies that the c axes of the grains are aligned along the film-normal direction. The full width at half-maximum intensity of the (001) peak rocking curve [inset of Fig. 1(c)] is about 2.9° , indicating the c axes are aligned quite well along the film-normal direction. The reason for this c -axis orientation is not clear, but presumably involves the growth mechanism of the ordered FePt crystallites; further investigations are in progress. The broadening of the (001) and (002) peaks indicates shorter coherence length normal to the film as the B_2O_3 layer thickness increases. The films with B_2O_3 layer thickness equal to 16 Å or larger retain a layered structure after annealing; an example of the low-angle XRD pattern is shown in the inset of Fig. 1(d).

The nanostructure of the annealed FePt/ B_2O_3 multilayers was investigated by TEM. Figure 2(a) is a bright field image of the 550 °C annealed (FePt 32 Å/ B_2O_3 12 Å)₅ multilayer. The FePt grain size was found in a wide range from 10 to 30 nm. As the B_2O_3 concentration increases, the grain size decreases. Figure 2(b) is a high resolution TEM image of the annealed (FePt 32 Å/ B_2O_3 20 Å)₅ multilayer. It shows that fine FePt single crystals about 4 nm in size were randomly dispersed in the B_2O_3 matrix.

Hysteresis loops were measured with applied fields both parallel and perpendicular to the film plane. For the FePt $L1_0$ phase, the c axis is the magnetic easy axis. Similar hysteresis loops were obtained in both directions for the FePt single-layer film and the (FePt 32 Å/ B_2O_3 8 Å)₅ multilayer, as shown in Figs. 3(a) and 3(b), which implies the random ori-

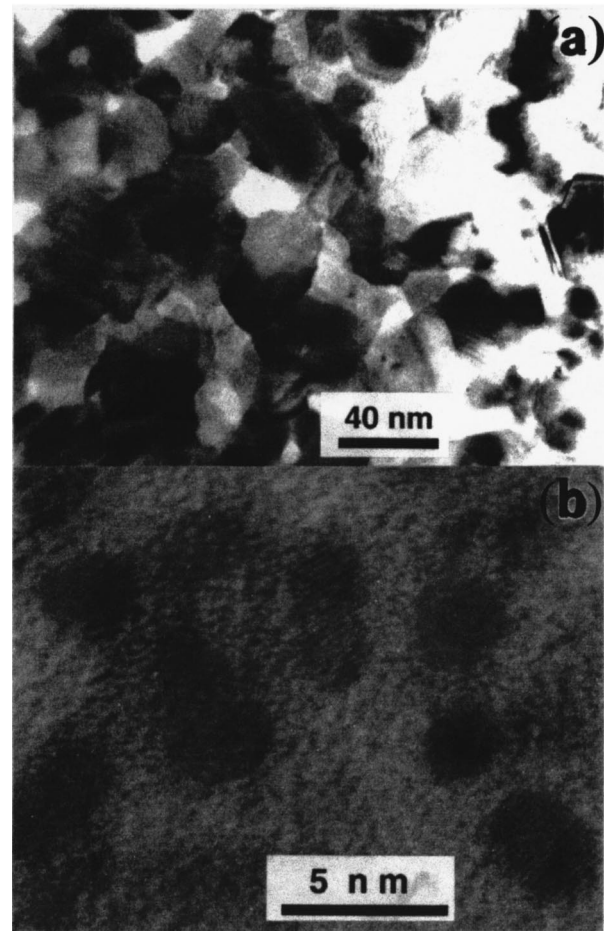


FIG. 2. TEM images of: (a) (FePt 32 Å/ B_2O_3 12 Å)₅, and (b) (FePt 32 Å/ B_2O_3 20 Å)₅ annealed at 550 °C for 30 min.

entation of the magnetic grains. When the B_2O_3 layer thickness increases to 12 Å and above, perpendicular anisotropy was observed, as shown in Figs. 3(c) and 3(d). The perpendicular loops show a remanence close to 100% of saturation

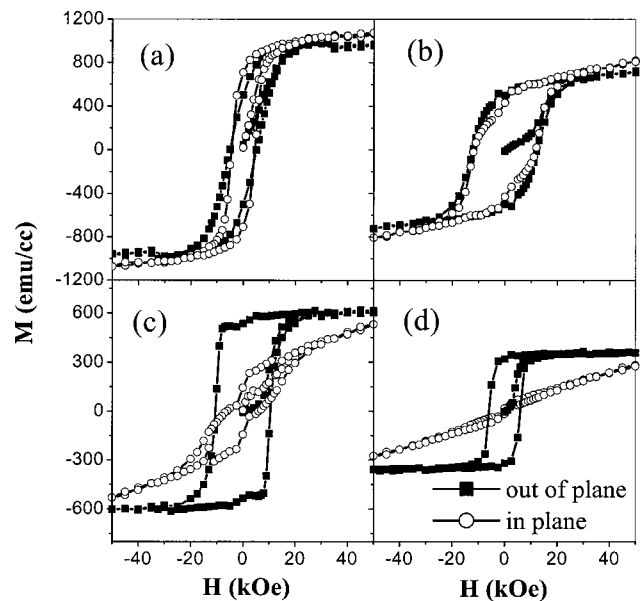


FIG. 3. Hysteresis loops of: (a) FePt single layer; (b) (FePt 32 Å/ B_2O_3 8 Å)₅; (c) (FePt 32 Å/ B_2O_3 12 Å)₅, and (d) (FePt 32 Å/ B_2O_3 48 Å)₅. These films were annealed at 550 °C for 30 minutes.

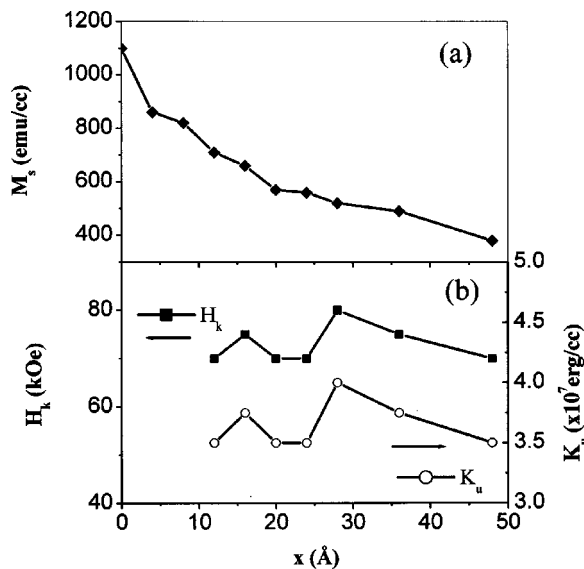


FIG. 4. The dependence of M_s , H_k , and K_u on the B_2O_3 layer thickness.

magnetization. The in-plane hysteresis loops diminish as the B_2O_3 layer thickness increases. This is consistent with the XRD measurements.

The saturation magnetization M_s of the films decreases as B_2O_3 thickness increases due to the increase of B_2O_3 concentration, as shown in Fig. 4(a). After normalization by the volume fraction of FePt, the M_s of the FePt phase in the FePt: B_2O_3 nanocomposites is about 1000 emu/cc, slightly less than the M_s (~ 1100 emu/cc) of the FePt single layer film. This might be due to the isolation of FePt grains by the B_2O_3 matrix, resulting in smaller moments for the atoms at the grain surface. By extrapolating the magnetization curves, the anisotropy field H_k and anisotropy energy $K_u = M_s H_k / 2$ were obtained, as shown in Fig. 4(b). The H_k values are around 70–80 kOe, which is close to the H_k value of the $Fe_{45}Pt_{55}$ thin film measured by Li and Lairson.¹⁰ With $M_s = 1000$ emu/cc, the K_u value is about $3.5\text{--}4.0 \times 10^7$ erg/cc.

The average grain size d was estimated by the Scherrer formula¹¹ from the (001) diffraction peak. The dependence of d and coercivity H_c on the B_2O_3 layer thickness are shown in Fig. 5. The average grain sizes are well below the critical single domain particle size (~ 300 nm). Since the coercivity is much smaller than the anisotropy field ($H_c/H_k < 0.2$), an incoherent reversal mechanism is suggested. As shown in Fig. 5, a small amount (up to 20 vol.%) of B_2O_3 sharply increases the coercivity from 5.2 to 12 kOe. At the same time, the grain size d only slightly changes. Therefore, the increase in coercivity might be due to the decrease of intergranular exchange coupling and/or the increase of the number of pinning sites when B_2O_3 is added. However, further increase of B_2O_3 results in the sharp decrease of H_c . This is probably due to the sharp decrease in grain size and thermal activation effect plays an important role in magnetization reversal when grain size is below 10 nm. When the B_2O_3 layer thickness reaches 28 Å and above, d remains a constant value, close to the FePt layer thickness. This is consistent with the low angle XRD scans which indicate that the film retains a layered structure after annealing.

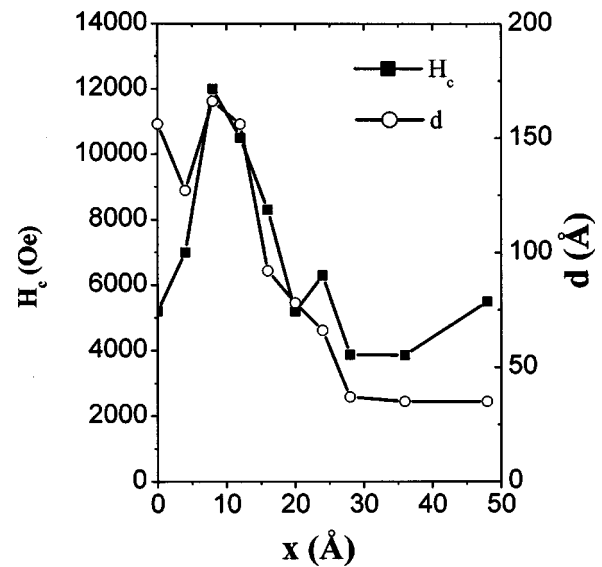


FIG. 5. The dependence of coercivity H_c and grain size d on the B_2O_3 layer thickness.

In summary, FePt: B_2O_3 nanocomposite thin films with strong perpendicular anisotropy were successfully fabricated on glass substrates. The fabrication of the films requires only conventional sputter-deposition and thermal-annealing processing. Under appropriate conditions these films consist of $L1_0$ FePt particles embedded in the B_2O_3 matrix with the c axes of the grains aligned along film normal direction. A high anisotropy energy was found, about 3.5×10^7 erg/cc. The grain sizes and coercivities were found to be dependent on the B_2O_3 layer thickness. These films have fine grain sizes (< 10 nm), adjustable coercivities (4–12 kOe), and perpendicular magnetic anisotropy, which suggest this nanocomposite system may have significant potential as recording media at extremely high areal densities.¹²

This research was supported by the DOE under Grant No. DOE-DE-FG-03-98ER45703. In addition Y.L. and D.J.S. benefited from the support of DARPA/ARO and AFOSR, and S.H.L. and L.G. were supported by ARO under Grant No. DAAG 55-98-1-0014, and from the support of CMRA and NRI at the University of Nebraska.

¹C. P. Luo and D. J. Sellmyer, IEEE Trans. Magn. **MAG-31**, 2764 (1995).

²K. R. Coffey, M. A. Parker, and J. Kent Howard, IEEE Trans. Magn. **MAG-31**, 2737 (1995).

³N. Li and B. M. Lairson, IEEE Trans. Magn. **MAG-35**, 1077 (1999).

⁴J. P. Liu, C. P. Luo, Y. Liu, and D. J. Sellmyer, Appl. Phys. Lett. **72**, 483 (1998).

⁵M. R. Visokay and R. Sinclair, Appl. Phys. Lett. **66**, 1692 (1995).

⁶R. F. C. Farrow, D. Weller, R. F. Marks, M. F. Toney, S. Hom, G. R. Harp, and A. Cebollada, Appl. Phys. Lett. **69**, 1166 (1996).

⁷O. A. Ivanov, L. V. Solina, V. A. Demshina, and L. M. Msgat, Phys. Met. Metallogr. **35**, 81 (1973).

⁸A. Cebollada, D. Weller, J. Sticht, R. Harp, R. F. C. Fallow, R. F. Marks, R. Savoy, and J. C. Scott, Phys. Rev. B **50**, 3419 (1994).

⁹R. F. C. Farrow, D. Weller, R. F. Marks, M. F. Toney, A. Cebollada, and G. R. Harp, J. Appl. Phys. **79**, 5967 (1996).

¹⁰N. Li and B. M. Lairson, J. Appl. Phys. **85**, 5142 (1999).

¹¹B. D. Cullity, *Elements of X-Ray Diffraction*, 2nd ed. (Addison-Wesley, Reading, MA, 1978), p. 102.

¹²R. Wood, IEEE Trans. Magn. **36**, 36 (2000).